

Pair interaction of charged colloidal spheres near a charged wall

Sven H. Behrens and David G. Grier

Department of Physics, James Franck Institute, and Institute for Biophysical Dynamics, The University of Chicago, Chicago, Illinois 60637

(Received 09 January 2001; published 18 October 2001)

Although equally charged colloidal particles dispersed in clean water are expected to repel each other, an unexplained long-range attraction has consistently been reported for charged colloidal spheres confined by charged macroscopic surfaces. We present an alternative equilibrium measurement of the pair interaction energy for charged spheres near a single charged wall. Analyzing their radial distribution functions for different concentrations reveals a purely repulsive sphere-sphere interaction that is well described by a screened Coulomb potential.

DOI: 10.1103/PhysRevE.64.050401

PACS number(s): 82.70.Dd, 05.40.-a, 61.20.-p

One of the most prominent open questions in colloid physics concerns the influence of spatial confinement on the interaction between charged colloidal particles. For an isolated pair of similar particles in an electrolyte solution, the classical Derjaguin-Landau-Verwey-Overbeek (DLVO) theory [1] predicts a short-ranged van der Waals interaction and an electrostatic repulsion, which, for well-separated spherical macroions, takes the familiar screened Coulomb form

$$u(r) = \frac{(Z^*e)^2}{\epsilon} \frac{\exp(\kappa\sigma)}{(1 + \kappa\sigma/2)^2} \frac{\exp(-\kappa r)}{r}. \quad (1)$$

Here, $u(r)$ is the electrostatic energy between spheres separated by r , each of diameter σ and carrying an effective charge number Z^* , dispersed in a medium of dielectric constant ϵ and Debye screening length κ^{-1} . Van der Waals attraction is negligibly weak at the sphere separation of interest [2] and is omitted from Eq. (1).

Experimentally, the pair interaction energy can be assessed by analyzing the relaxation of two particles released from optical traps [3,4], or by interpreting the liquid structure of an equilibrated dispersion [5–7]. Both techniques consistently reveal that polystyrene spheres dispersed in deionized water and closely confined between parallel glass walls experience a long-range pair attraction [6–9] qualitatively inconsistent with DLVO predictions, and more generally with mean-field [10] or local density theories [11]. Unconfined particles, on the other hand, repel each other as expected [3,5,8],

This Rapid Communication reports measurements of colloidal pair interactions in equilibrium near a single wall. The only previous one-wall measurement used optical tweezers to position highly charged polystyrene spheres near a charged glass surface, and then released the spheres to measure their interactions [12]. Although this measurement revealed attractions consistent with those observed between two walls, Squires and Brenner [13] showed that they could have resulted from hydrodynamic flows excited by the spheres' retreat from the wall, a purely kinematic effect. The resulting hydrodynamic interaction would mask any other attraction in nonequilibrium measurements near a single

wall. It cannot have influenced the equilibrium long-ranged attractions deduced from the structure of colloidal monolayers confined between two walls [6,7]. Nor does it account for the anomalous attractions measured with optical tweezers between two walls; reanalyzing the data from Ref. [8] reveals no sign of hydrodynamic memory. Moreover, indirect evidence based on the structure and dynamics of metastable crystals [12,14] suggests that a single wall can induce like-charge attractions in suspensions of sufficiently low ionic strength. Our measurements therefore focus on this regime.

Our samples consists of monodisperse silica spheres ($\sigma = 1.58 \mu\text{m}$, Catalog No. 8150, Duke Scientific, Palo Alto, CA) dispersed in deionized water and confined in the gap between a No. 1 glass coverslip and a glass microscope slide, as shown in Fig. 1. The spheres and bounding glass walls acquire negative surface charges by dissociation of silanol groups. The sample volume is sealed with a high-purity UV cured adhesive (Norland Type 88), using pieces of a second coverslip as spacers. The enclosed volume is roughly $200\text{-}\mu\text{m}$ thick. Two glass tubes extending from holes drilled through the slide provide access to the sample volume. After filling, they serve as reservoirs for mixed-bed ion exchange resin to maintain low ionic strength, and are sealed with

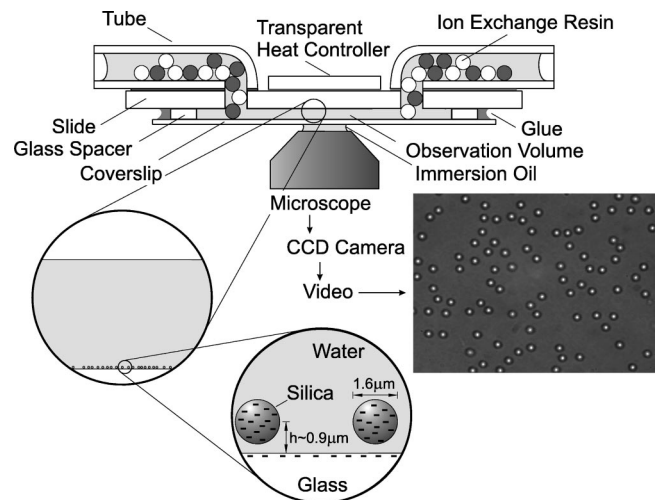


FIG. 1. The experimental setup together with a typical video image of the $70 \times 52 \mu\text{m}^2$ field of view.

rubber tubes and glass plugs. All glass surfaces were cleaned prior to assembly with a 1:3 mixture of hydrogen peroxide and concentrated sulfuric acid, and copiously rinsed in hot deionized water. This preparation reproducibly yields $\kappa\sigma \approx 10$ at the experimental temperature of $29.0 \pm 0.1^\circ\text{C}$.

Because of their high specific mass (2.2 g/cm^3), the particles sediment to the bottom wall in a matter of minutes, reaching an equilibrium height $h = 0.9 \pm 0.1 \mu\text{m}$, where the force due to gravity is balanced by the spheres' electrostatic interaction with the wall's surface charge. The spheres' unvarying appearance under the microscope confirms their out-of-plane excursions to be smaller than $0.1 \mu\text{m}$. Limited out-of-plane motion reduces the possibility of projection errors, which have been identified [15] as a concern in earlier studies.

The particles were observed with an inverted optical microscope (Olympus IMT-2), using a $100\times$ N.A. 1.4 oil immersion objective and a $2.5\times$ video eyepiece. These image an area $A = 70 \times 52 \mu\text{m}^2$ in the 640×475 pixel field of view of an attached charge-coupled device camera. The particles' motions were recorded at 30 frames per second before being digitized with a (MuTech MV-1350) frame grabber. Standard image analysis techniques [4] were used to locate the spheres to within 30 nm.

Following the principle adopted in earlier studies, we measure the spheres' pair potential by compiling histograms of equilibrium pair separations into the two-dimensional pair correlation function, $g(r)$. In the limit of infinite dilution, $g(r)$ is related to the pair interaction energy through the Boltzmann distribution, $\lim_{n \rightarrow 0} g(r) = \exp[-u(r)/k_B T]$, where n is the areal density of spheres. For finite concentration, on the other hand, the radial distribution function also reflects neighboring particles' influence, and generally

$$w(r) = -k_B T \ln g(r) \quad (2)$$

is the potential of mean force [16]. While no exact relationship is known between the experimentally accessible $w(r)$ and its underlying pair potential $u(r)$, accurate approximations are available [16] provided that $g(r)$ is measured with sufficient precision.

Although straightforward in principle, imaging measurements of $g(r)$ are subject to subtle sources of error that can introduce spurious features into $u(r)$. These errors arise principally from three sources: truncation by the limited field of view, statistical undersampling of suspensions' slow dynamics, and uncorrected many-body correlations. Previous reports have addressed some, but not all, aspects of these errors [5–7]. Consistency among their results reinforces their qualitative conclusions, while leaving some doubt regarding their quantitative accuracy. For this reason, we outline our methods.

The pair correlation function measures the mean number $ng(\vec{r})$ of particles per unit area separated from any given sphere by displacement \vec{r} . This average is calculated in practice by counting the number of \vec{r} pairs in a recorded image and normalizing by the number of particles actually tested for a partner at separation \vec{r} , i.e., by the number of particles

in the ‘‘overlap area’’ $A \cap (A - \vec{r})$, where A is the set of points in the field of view and $(A - \vec{r})$ is the same set displaced by \vec{r} . Summing over angles yields $2\pi r n g(r) dr$, and hence $g(r)$.

The field of view in Fig. 1 contains too few particles to sample $g(r)$ accurately. Increasing the field of view to improve statistics would degrade particle tracking performance [4]. Consequently, results from independent images must be averaged to improve statistics. Unless the particles are given time to redistribute between snapshots, however, these additional images will not shed light on the suspension's equilibrium properties so much as improve the sampling of a particular transient distribution. The need for statistically independent samples implies that the period over which $g(r)$ is averaged must be chosen with care.

If the monitored area A were so large that edge effects could be neglected, then a histogram of the particle separations with bin width δ would give $g(r)$ as the average number of particles separated by distance $r \pm \delta/2$ from any given particle, normalized by the corresponding value $2\pi n r \delta$ for an ideal system of noninteracting particles. Given $N(r)$ pairs at separation r in a snapshot,

$$g(r) = N(r) / (\pi n^2 r \delta A). \quad (3)$$

In practice, $N(r)$ tends to be of order unity, while $N(r) > 1/\Delta$ would be required to sample $g(r) \approx 1$ to a relative accuracy of Δ . Achieving this accuracy near contact requires a minimum of $M = (\Delta \pi \sigma \delta A n^2)^{-1}$ uncorrelated snapshots. The interval between snapshots is limited by the decay of correlations, and thus is proportional to the time $\tau = (4Dn)^{-1}$ a particle needs to diffuse the mean interparticle distance $n^{-1/2}$ given its diffusion constant D . The total time needed to sample $g(r)$ therefore scales as $M\tau \propto n^{-3}$.

Because the experimental duration increases so rapidly with dilution and because controlling concentration, temperature, and ionic strength over long periods can be difficult, statistical accuracy strongly favors larger particle concentrations. On the other hand, extracting the pair potential from measured correlations becomes increasingly difficult as n increases. The areal densities between $n\sigma^2 = 0.05$ and 0.1 chosen for this study require no more than a 30-min sampling and represent a compromise between statistical and interpretive accuracy.

Our experimental results for $g(r)$ and $w(r)$ at different concentrations are shown in Fig. 2. The curves indicate a repulsive core interaction causing particle depletion from a zone about 2σ wide. Beyond this is a preferred nearest-neighbor separation between 2σ and 3σ and the oscillatory correlations typical of a structured fluid. The depth of the minimum in $w(r)$ clearly depends on n , and so reflects at least some many-body contributions.

To ensure that none of the observed correlations result from inhomogeneities in the glass surface's properties, we compared two-dimensional histograms of recorded particle positions with analogous histograms for uniformly distributed random data sets. Differences in these histograms' first two moments vanish with increasing delay time, confirming that each particle's position becomes uncorrelated over time

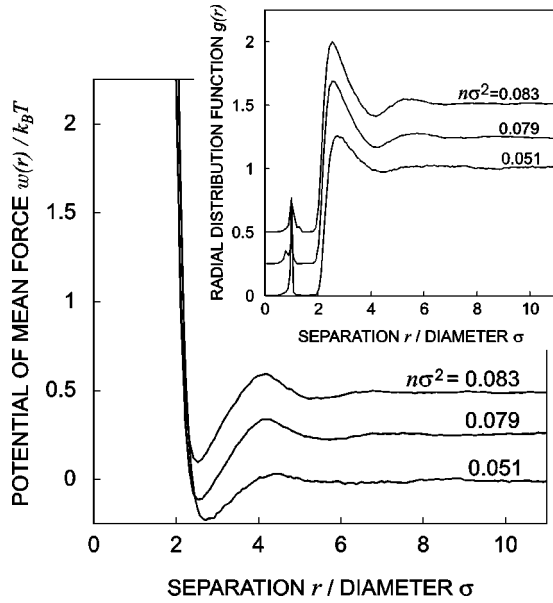


FIG. 2. The measured potential of mean force for three different particle concentrations, obtained from the inset radial distribution functions. Curves are offset by 0.25 for clarity. Spurious correlations at $r=\sigma$ arise from a small number of aggregated dimers and were disregarded in the analysis.

as expected. Thus the substrate potential appears to be featureless on the length- and time scales of our experiment, to within our resolution.

Provided that $g(r)$ is free from experimental artifacts, reliable approximations for $u(r)$ can be obtained from $w(r)$ using the Ornstein-Zernike integral equation with appropriate closure relations. Good results for “soft” potentials are typically achieved with the hypernetted chain (HNC) approximation, whereas the Percus-Yevick (PY) approximation is known to be a better choice for hard spheres. The pair interaction potential can be evaluated numerically in these approximations as

$$u(r) = w(r) + \begin{cases} nk_B T I(r) & \text{(HNC)} \\ k_B T \ln[1 + nI(r)] & \text{(PY)} \end{cases} \quad (4)$$

where the convolution integral

$$I(r) = \int [g(r') - 1 - nI(r)][g(|\mathbf{r}' - \mathbf{r}|) - 1] d^2 r' \quad (5)$$

can be solved iteratively, starting with $I(r)=0$ [17]. Evaluating $I(r)$ directly rather than with numerical Fourier transforms minimizes the sensitivity of $u(r)$ to noise in $g(r)$. Results for $n\sigma^2=0.051$ appear in Fig. 3. Corresponding results for $n\sigma^2=0.079$ and 0.083 are essentially indistinguishable.

The absence of minima in the pair potential confirms that crowding induces the observed oscillations in $w(r)$, while the underlying interaction is purely repulsive. The solid curves in Fig. 3 are fits to Eq. (1) for Z^* , κ , and an arbitrary additive offset. The fitting parameters listed in Table I are

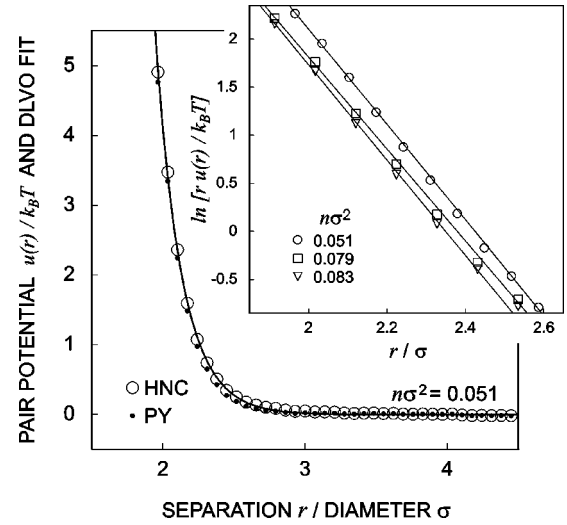


FIG. 3. The pair interaction energy calculated from the potential of mean force (Fig. 2) in the HNC approximation (open circles) together with a fit to Eq. (1). Equivalent results in the Percus-Yevick approximation are shown as full dots. Inset: Logarithmic representation of HNC results and best fits to Eq. (1) for data obtained at different areal densities.

consistent with surface charging due to silanol dissociation at an ionic strength around 10^{-6} M [18].

The DLVO theory’s success at characterizing our data might seem surprising given the experimental geometry. However, the DLVO form has been shown to capture the leading-order behavior for confined colloidal interactions in the Poisson-Boltzmann approximation, with the bounding wall introducing only an additional dipole repulsion [19,20] to lowest order. The dipole correction is predicted [20] to be weaker than our $0.1 k_B T$ experimental resolution over the experimentally accessible range of interparticle separations. Long-range attractions of the previously reported strength [6–8,12] would have been resolved.

A dynamic aspect of the observed particle correlations is illustrated by the van Hove function, plotted in Fig. 4 for $n\sigma^2=0.051$. This function is defined by [16]

$$G(\vec{r}, t) = \left\langle N^{-1} \sum_{j,k=1}^N \delta[\vec{r} + \vec{r}_j(0) - \vec{r}_k(t)] \right\rangle, \quad (6)$$

where $\vec{r}_j(t)$ is the position of particle j at time t . The partial sum for $j=k$, known as the self part $G_s(\vec{r}, t)$ of the van Hove function, describes the correlation of one particle’s positions at different times; initially localized at the origin, $G_s(\vec{r}, 0)$

TABLE I. Charge numbers and screening lengths obtained from fits of Eq. (1) to the data in Fig. 3.

$n\sigma^2$	Z_{HNC}^*	Z_{PY}^*	$\kappa_{\text{HNC}}^{-1} (\mu\text{m})$	$\kappa_{\text{PY}}^{-1} (\mu\text{m})$
0.051	5504	6502	0.32	0.30
0.079	4312	5603	0.33	0.30
0.083	4656	6039	0.32	0.29

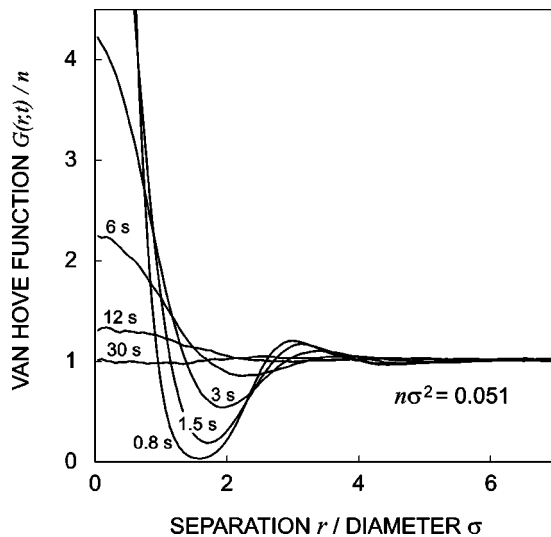


FIG. 4. Time slices of the van Hove function $G(r,t)$.

$= \delta(\vec{r})$, this function broadens as the particles diffuse. The remaining sum over pairs of different particles ($j \neq k$), called the distinct part $G_d(\vec{r}, t)$, describes the progressive fading of the initial pair correlation $G_d(\vec{r}, 0) = ng(r)$. If the pair correlation peak (at around 3σ) were due to attractive particles diffusing as a pair, one should expect this peak to be more

persistent than the self-correlation peak (at $r=0$). In the present case both peaks flatten out simultaneously.

The decay of $G_s(0,t)$ provides an estimate [16] of $\tau = 35$ sec for the sample with $n\sigma^2 = 0.051$. The 30-min measurement period therefore yields $g(r)$ with a relative error $\Delta = 0.026$, given our binning resolution $\delta = 100$ nm. The other samples yield comparably good results.

The absence of a measurable interparticle attraction in this experiment should be interpreted with care. Our silica spheres carry lower charge densities than the polystyrene particles used in earlier studies, and the sphere-wall separation is considerably smaller. A wall-induced equilibrium attraction that depended at least linearly on charge would have been weaker than our experimental resolution. The measured structure of our colloidal monolayers suggests instead that like-charged particles repel each other in pure water, even near a charged wall. Our observations support the electrohydrodynamic explanation [13] for the attraction measured with optical tweezers in Ref. [12], thus distinguishing that attraction from those seen in dispersions confined between two walls, and those implicated in observed anomalous phase behavior in bulk suspensions.

We are grateful to Todd Squires, Michael Brenner, and Vladimir Lobaskin for enlightening conversations. This work was supported by the National Science Foundation through Grant No. DMR-9730189 and by the Swiss National Science Foundation.

- [1] B.V. Derjaguin and L. Landau, *Acta Physicochim. URSS* **14**, 633 (1941). E. J. Verwey and J. T. G. Overbeek, *Theory of the Stability of Lyophobic Colloids* (Elsevier, Amsterdam, 1948).
- [2] B.A. Pailthorpe and W.B. Russel, *J. Colloid Interface Sci.* **89**, 563 (1982).
- [3] J.C. Crocker and D.G. Grier, *Phys. Rev. Lett.* **73**, 352 (1994).
- [4] J.C. Crocker and D.G. Grier, *J. Colloid Interface Sci.* **179**, 298 (1996).
- [5] K. Vondermassen, J. Bongers, A. Mueller, and H. Versmold, *Langmuir* **10**, 1351 (1994).
- [6] G.M. Kepler and S. Fraden, *Phys. Rev. Lett.* **73**, 356 (1994).
- [7] M.D. Carbajal-Tinoco, F. Castro-Román, and J.L. Arauz-Lara, *Phys. Rev. E* **53**, 3745 (1996).
- [8] J.C. Crocker and D.G. Grier, *Phys. Rev. Lett.* **77**, 1897 (1996).
- [9] M.D. Carbajal-Tinoco, G. Cruz de León, and J.L. Arauz-Lara, *Phys. Rev. E* **56**, 6962 (1997).
- [10] J.C. Neu, *Phys. Rev. Lett.* **82**, 1072 (1999); J. E. Sader and D. Y. C. Chan, *J. Colloid Interface Sci.* **213** 268 (1999); E. Trizac and J.-L. Raimbault, *Phys. Rev. E* **60**, 6530 (1999).
- [11] E. Trizac, *Phys. Rev. E* **62**, 1465 (2000).
- [12] A.E. Larsen and D.G. Grier, *Nature (London)* **385**, 30 (1997).
- [13] T. Squires and M.P. Brenner, *Phys. Rev. Lett.* **85**, 4976 (2000).
- [14] A.E. Larsen and D.G. Grier, *Phys. Rev. Lett.* **76**, 3862 (1996).
- [15] K.S. Rao and R. Rajagopalan, *Phys. Rev. E* **57**, 3227 (1998).
- [16] J.-P. Hansen and I. R. McDonald, *Theory of Simple Liquids*, 2nd ed. (Academic Press, London, 1986).
- [17] E.M. Chan, *J. Phys. C* **10**, 3477 (1977).
- [18] S.H. Behrens and D.G. Grier, *J. Chem. Phys.* (to be published).
- [19] F.H. Stillinger, *J. Chem. Phys.* **35**, 1584 (1961); A.J. Hurd, *J. Phys. A* **18**, L1055 (1985).
- [20] R.R. Netz and H. Orland, *Eur. Phys. J. E* **1**, 203 (2000).